

Recombination processes in a highly charged ion beam extracted from a laser ion source.

G. Hall, S. Kondrashev, H. Kugler, R. Scrivens,
B. Sharkov, R. Sherwood, J. Tambini

1 Abstract

The experimental results of highly charged ion beam transport with space charge compensation by electrons are presented. A tungsten thermionic cathode has been used as a source of electrons for ion beam space charge compensation. An enhancement factor in ion current density of 8 - 10 is obtained for an extraction voltage of 40 kV, while a factor of 3 - 5 is obtained for an extraction voltage of 60 kV. The transport distance was 1.2 m. Special attention is given to recombination processes in an ion beam with a high degree of compensation. Charge states and energy distributions were deduced from the beam distributions measured with a micro-channel plate (MCP), with a phosphor screen and CCD-camera, after the bending magnet. Significant recombination, for highly charged ions, was observed due to the thermoelectrons.

2 Background - recombination processes

Studying recombination processes is interesting from two points of view.

Firstly, it can lead to an understanding of the distribution of charge states and energy seen in extracted ion beams. It has been shown [1] that a considerable number of ions ($>10\%$) have their charge state reduced during a flight of some meters after extraction and acceleration (“recombination ions”). The number of “recombination ions” cannot be explained by either charge exchange with molecules of the residual gas (for pressures less than

$3 \cdot 10^{-6}$ Torr) or atoms produced by the ion beam striking the walls. The process described below seems the most probable cause of recombination. Secondary electrons released from the walls of the vacuum chamber are captured by the electric field of the ion beam. Potential differences in the ion beam may be several kV for ion beam currents of ≈ 100 mA. Recombination processes can take place in such an ion beam with some degree of space charge compensation due to the electrons. Studying the charge state and energy distributions in an ion beam with a high degree of compensation is important in understanding such recombination processes and suggesting means to avoid them.

Secondly, space charge compensation by electrons may have use in different schemes of ion beam transport.

3 Experimental set-up

The arrangement of the experiment is shown in Fig.1. The tantalum ion beam was extracted from a laser produced plasma by a three electrode system with apertures of 3 cm diameter. The extraction system was placed at a distance of 108 cm from the target. The extracted ion beam was allowed to drift 3.4 m downstream to the magnetic spectrometer. The entrance slit of the spectrometer had a width of 0.75 mm. The MCP, with a phosphor screen and CCD, was placed behind the exit slit which was opened to 37 mm.

The ion beam current was measured with a Faraday cup with two grids at the entrance. This cup was first placed at a distance of 1.2 m downstream of the extraction system. The first grid was grounded and the second, which was upstream, was set to a potential of -1 kV. This allowed the Faraday cup to register the ion current only (ions and electrons were separated at the cup entrance). The secondary electrons from the grid nearest the final collector can be neglected due to the high transparency of the grids.

The electron source was placed as close as possible to the outlet of the final electrode in the extraction system (5 cm downstream). The electron source consisted of a thermionic cathode in the form of 200 μ m diameter tungsten wire together with a grid positioned between the extraction system and the cathode. This was held at a negative potential (approx. -1 kV). The cathode configuration is shown in Fig.2. The wires were heated with a pulse current generator for 1 s. This period was determined by the time required

for the cathode to reach a steady emission rate. Pulse shapes for the heating current, thermionic current and the laser trigger are shown in Fig.3. The role of the negative grid near the electron emitter is to prevent electrons returning to the extraction region.

4 Experimental results

4.1 Faraday cup Measurements

Ion current signals from the Faraday cup are shown in Fig.4 and 5. In Fig.4 the thermionic source is off while in Fig.5 it is on. The upper trace is the signal from the thermionic cathode indicating the current of electrons leaving the cathode.

An increase in the current due to multicharged ions with $z_{av} = 20$ (arrival time at the cup 4 - 10 μ s after the laser shot) could be obtained by varying the negative potential at the grid and the cathode temperature. An increase of ion beam current, measured with the Faraday cup, by a factor of 8 - 10 with an extraction potential of 40 kV, and by a factor of 3 - 5 with an extraction potential of 60 kV, was obtained as a result of space charge compensation by thermoelectrons at a distance of 1.2 m from the extraction system.

It should be noted, that the reproducibility of the Faraday cup signals was not good. Moreover, when the electron source was on, voltage breakdown in the extraction system occurred frequently. Some stabilization with respect to breakdowns could be achieved by decreasing the potential of the intermediate electrode of the extraction system from -10 kV to -20 kV.

4.2 Distribution of ion charge state

CCD-images are shown in Fig.6 for $z = 11$, with the the electron source both off and on. Analogous images for $z = 18$ are shown in Fig.7. Integrated plots of CCD-images for $z = 10, 11, 18$ and 23 are shown in Figs.8, 9, 10 and 11, for the electron source both off and on. Calculated (solid line) and measured (dashed line) positions of recombined peaks are also indicated.

1. Analysis of these images show a small reduction in ion energy when the electron source is on. Such a decrease corresponds to a drop of extraction voltage in the range of 0 - 2.6 kV per charge state for different

shots depending on the charge state observed. This drop of extraction voltage may be due to a high current of thermoelectrons passing through the extraction region.

2. Currents for all charge states increase by a factor of 1.5 - 5, when the electron source is on. This is a consequence of decreasing the ion beam space charge repulsion due to the high degree of beam compensation by thermoelectrons.
3. For charge states $z = 10$ and 11 , the resolution is sufficient to identify a number of peaks. The calculation of the positions of these peaks indicates that such ions were accelerated in the extraction system as charge states $z + n$ ($n = 1, 2, \dots$) and they were analyzed by the magnet as $z + n - k$ ($k = 1, 2, \dots$) (chains $z + n - z + n - k$). The positions of such peaks were calculated with respect to the main charge state, accounting for the drop in extraction voltage (see item 1). It can be seen, that only one additional peak is registered for $z = 10$ and $z = 11$ in the absence of thermoelectrons. These peaks correspond to changes of charge state from 12 to 11 and 13 to 12 respectively. Recombination peaks for values of n up to 3 are observed with thermoelectrons in the beam. Corresponding processes are marked in Fig.8 and 9. Significant recombination is observed as a result of ion beam space charge compensation by thermoelectrons.

There is some discrepancy between the calculated and measured position of recombined peaks, probably caused by two effects a) the temporal dependence of the drop in extraction voltage and b) aberrations in magnetic field at the exit of the spectrometer.

4. CCD-images for $z = 18$ and $z = 23$ should consist of many peaks, but there is insufficient resolution to identify them.

5 Discussion of experimental results

As the first experiments show, significant recombination occurs when the space charge effect is compensated by thermoelectrons. This fact confirms that the cause of the lowering of some charge states in the ion beam is due to recombination of ions in the presence of secondary electrons, which are

captured by the ion beam electric field. It is necessary to take this effect into account when using space charge compensation in beam transport lines for highly charged ions, because the rates of all recombination processes strongly increase with z .

It is interesting, that the high recombination rates observed in these experiments do not agree with estimates based on treating a highly compensated beam as a plasma with appropriate electron temperatures ($T = 0.2 - 100$ eV). A possible mechanism in this case might involve the “selection” of ions by electrons (with respect to ion velocity) during their oscillations in the beam potential along beam axis. This selection may occur because at some times a group of electrons may have a very small velocity (close to the natural dispersion of ion velocity in the beam) with respect to a group of ions. Resonant three-body recombination might be realized in this case.

Further experiments are needed to obtain more quantitative information about recombination processes and to understand their nature. The aims of such experiments should be:

1. The improvement of reproducibility of results from shot to shot and to decrease the risk of breakdowns in the extraction system;
2. The improvement in resolution of charge states by a better positioning of the MCP. (In these experiments the MCP was placed at the distance of 30 cm behind the focal plane of the beam optical system);
3. The identification of the numbers of recombined ions for all processes $(z + n)$ to $(z + n - k)$ for $(n, k = 1, 2, \dots)$ in the following cases:
 - thermoelectrons in the beam,
 - without thermoelectrons in the beam;
4. The estimation of the degree of space charge compensation for the ion beam:
 - by secondary electrons,
 - by thermoelectrons.

6 References

- [1] G. Belajev, V. Dubenkov, A. Golubev, B. Sharkov, A. Shumshurov, T. Henkelmann, G. Korschmeck, B. Wolf, D.H.H. Hoffmann, *Laser Plasma Ion Sources for Intense Heavy Ion Beams*, GSI Report (1992).

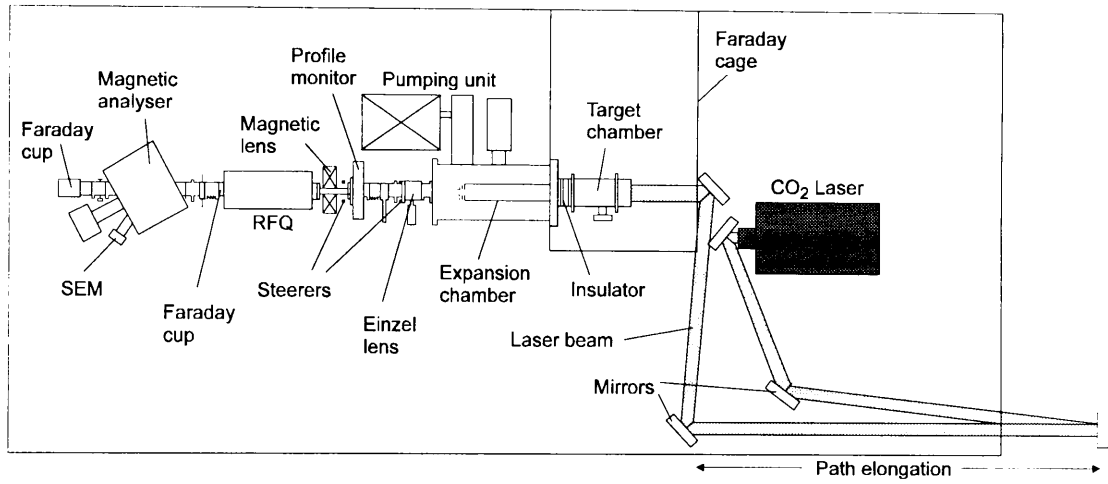


Fig 1. Schematic diagram of the Laser Ion Source experimental set-up.

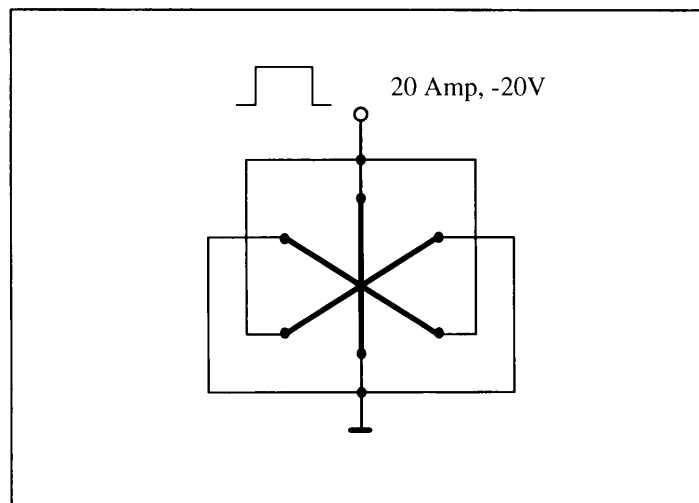


Fig 2. Thermionic cathode configuration.

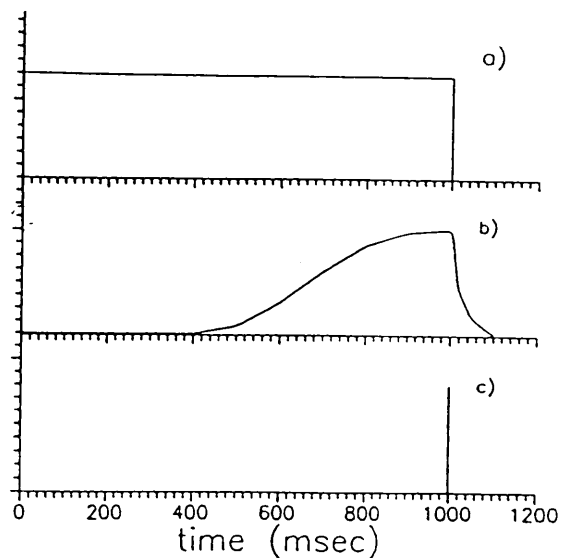
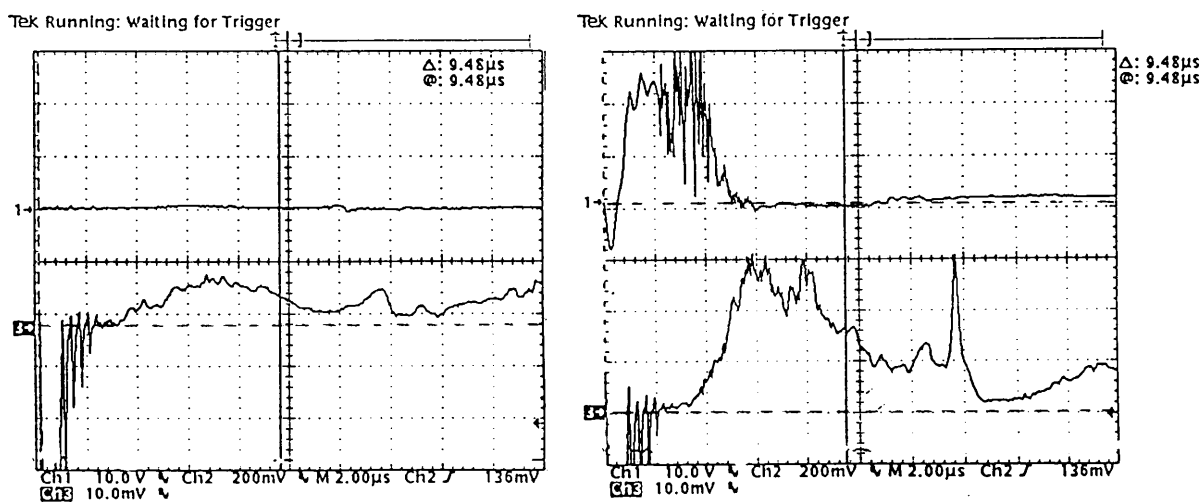


Fig. 3. a) Heating current, b) Thermionic current, c) Laser trigger.



Figs. 4 (left) and 5 (right). Trace 1 - Thermoelectron current. Trace 3 - Faraday cup signals, without (left) and with (right) thermionic cathode heating. Positive extraction voltage, $U_{ext}=60\text{kV}$; intermediate extraction voltage $U_{ii}=-20\text{kV}$; Faraday cup grid potential $U_{gFC}=-1\text{kV}$; thermionic cathode grid potential, $U_g=-1.5\text{kV}$.

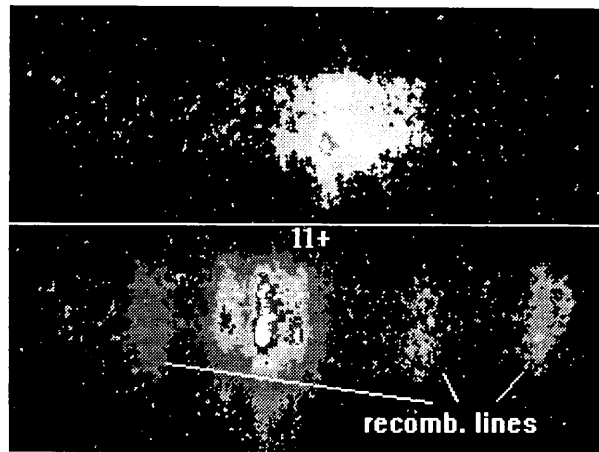


Figure 6. CCD images for $Z=11$; above - electron source off, below - electron source on.

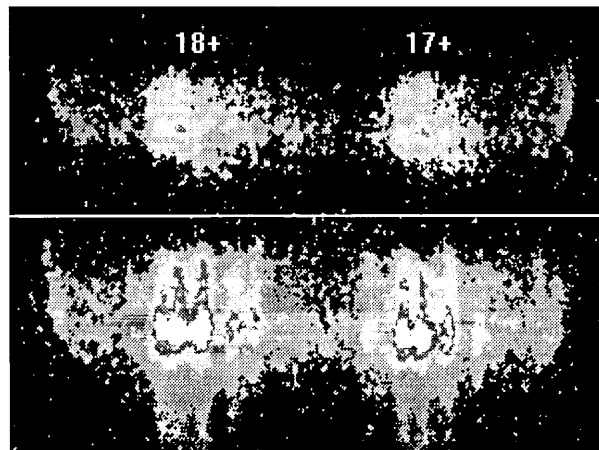


Figure 7. CCD images for $Z=18$; above - electron source off, below - electron source on.

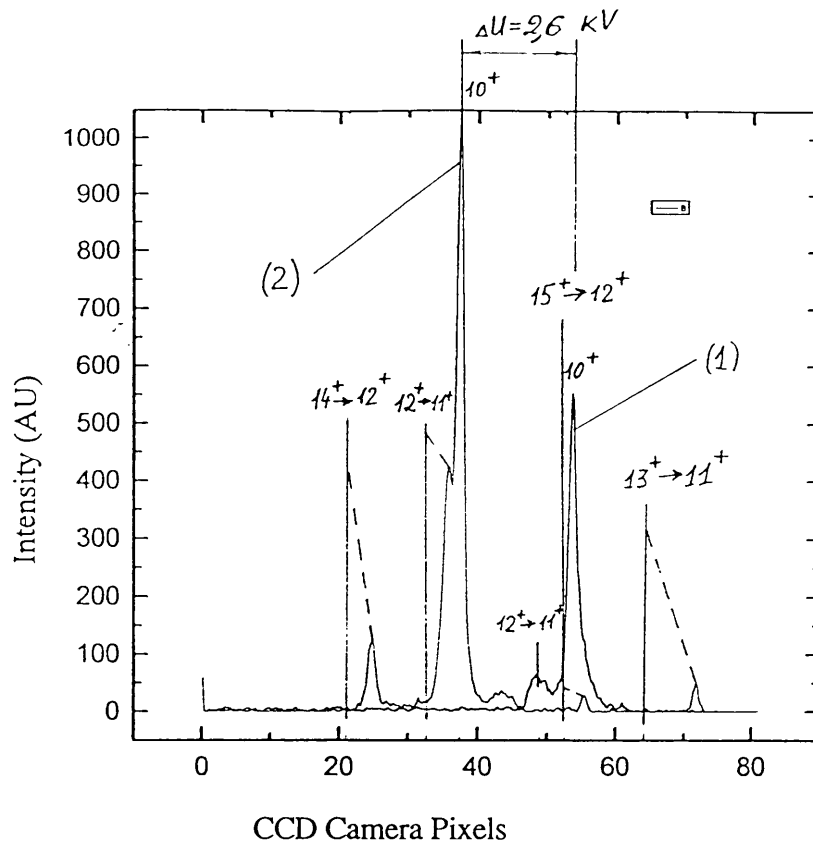


Fig. 8. Integrated plot of CCD Image around $z=10$. Trace 1 without thermoelectrons, Trace 2 with thermoelectrons.

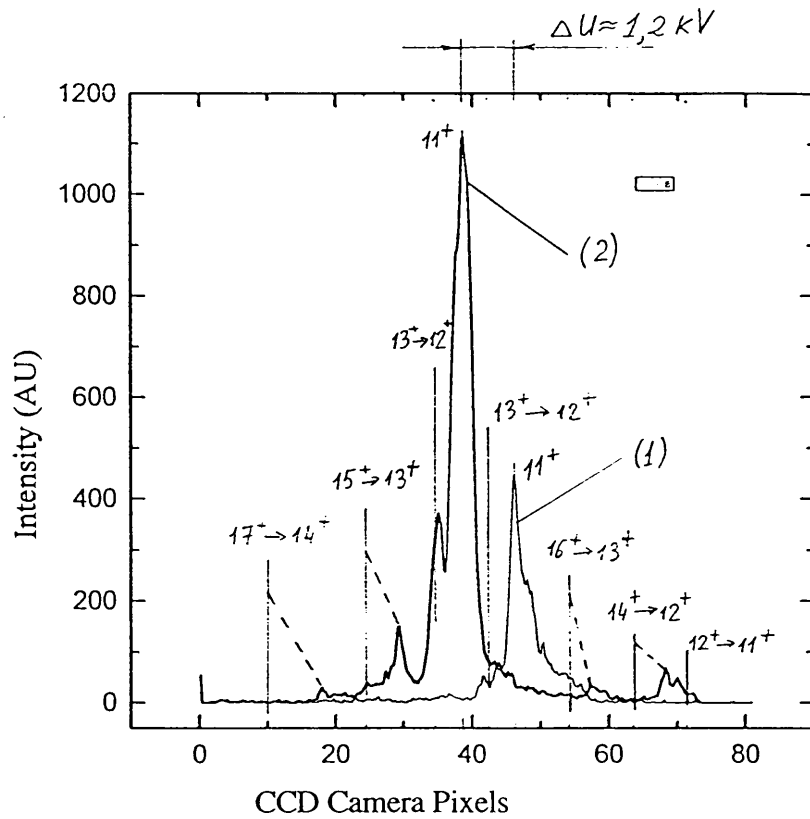


Fig. 9. Integrated plot of CCD Image around $z=11$. Trace 1 without thermoelectrons, Trace 2 with thermoelectrons.

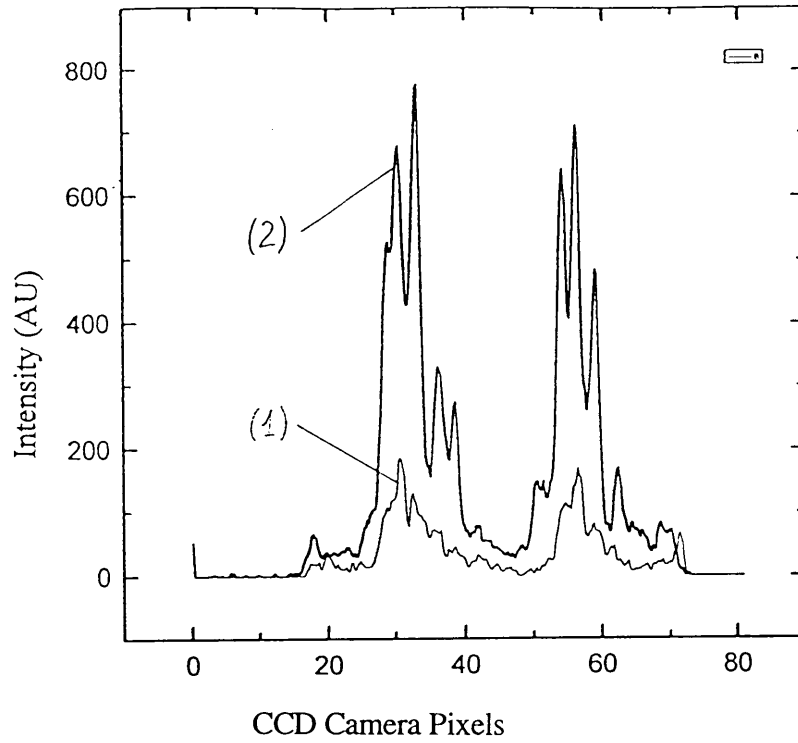


Fig. 10. Integrated plot of CCD Image around $z=18$. Trace 1 without thermoelectrons, Trace 2 with thermoelectrons.

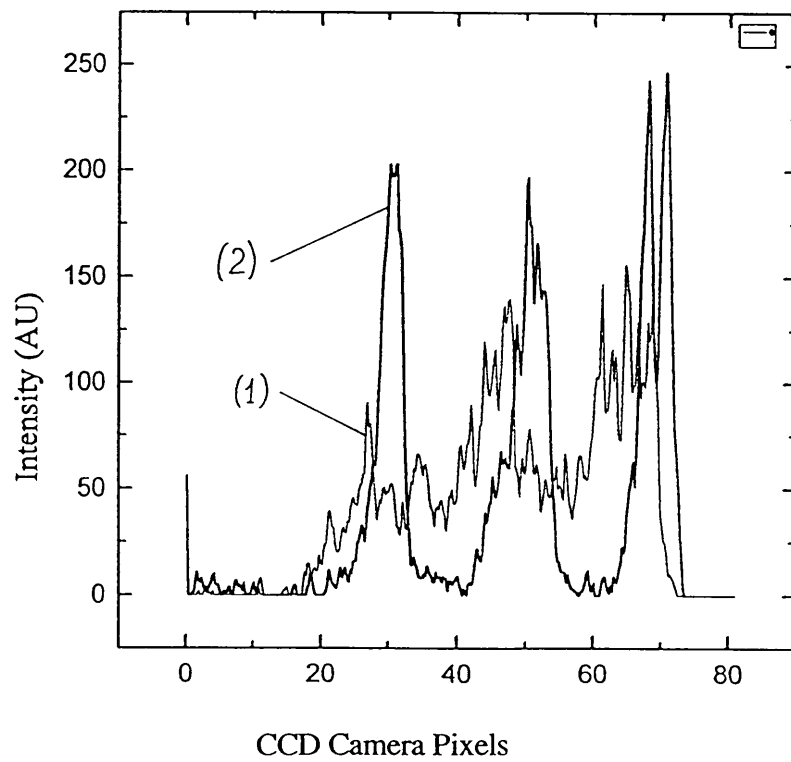


Fig. 11. Integrated plot of CCD Image around $z=23$. Trace 1 without thermoelectrons, Trace 2 with thermoelectrons.